Modeling corewood–outerwood transition in loblolly pine using wood specific gravity

Christian R. Mora, H. Lee Allen, Richard F. Daniels, and Alexander Clark

Abstract: A modified logistic function was used for modeling specific-gravity profiles obtained from X-ray densitometry analysis in 675 loblolly pine (*Pinus taeda* L.) trees in four regeneration trials. Trees were 21 or 22 years old at the time of the study. The function was used for demarcating corewood, transitional, and outerwood zones. Site and silvicultural effects were incorporated into the model. Heteroscedasticity and within-group correlation were accounted for by specifying the variance and serial-correlation structure, respectively. The estimated transition zone was located between rings 5 and 15, and the outerwood demarcation point varied from rings 12 to 15. No effects of treatments on the demarcation points were observed; however, site preparation and fertilization affected the lower asymptotes of the curves in all sites. A geographical trend for the demarcation point was observed, with the northern site requiring more time to reach a plateau in specific gravity compared with the southern sites. The diameter of the juvenile core was increased as a result of the treatments. However, the amount of corewood was not statistically affected, ranging from 55% in the north to 75% in the south, except at one site where fertilization decreased the percentage of corewood.

Résumé : Une fonction logistique modifiée a été utilisée pour modéliser les profils de densité obtenus par densitométrie chez 675 pins à encens provenant de quatre essais de régénération. Les arbres avaient 21 ou 22 ans au moment de l'étude. La fonction a été utilisée pour différencier les zones de bois juvénile, de bois de transition et de bois adulte. Les effets de la station et de la sylviculture ont été incorporés dans le modèle. En spécifiant la structure de la variance et de l'autocorrélation, on a respectivement tenu compte de l'hétéroscédasticité et de la corrélation dans les groupes. On a estimé que la zone de transition était située entre les cernes 5 et 15 et que le point de démarcation du bois adulte variait entre les cernes 12 à 15. Les traitements n'ont eu aucun effet sur les points de démarcation. Cependant, la préparation de terrain et la fertilisation on affecté l'asymptote inférieure des courbes dans toutes les stations. Une tendance géographique a été observée au sujet du point de démarcation : la densité prenait plus de temps pour atteindre un plateau dans la station située au nord que dans les stations plus au sud. Les traitements ont augmenté le diamètre du cœur juvénile. Cependant, la quantité de bois juvénile n'a pas été statistiquement affectée, variant de 55 % au nord à 75 % au sud, à l'exception d'une station où la fertilisation a entraîné une diminution du pourcentage de bois juvénile.

[Traduit par la Rédaction]

Introduction

The forest industry faces many challenges. Because of economic pressure for a continuing wood supply, the current plantations of loblolly pine (*Pinus taeda* L.) are largely under intensive management regimes. As forest management becomes more intensive (e.g., site preparation, fertilization, and weed control), trees will attain merchantable size at younger ages possibly resulting in material having different wood characteristics and properties compared with older ages. Future plantations that reach merchantability at younger ages will most likely contain a higher proportion of "juvenile wood" (Plomion et al. 2001).

Juvenile or inner corewood has been defined as the zone of wood extending outward from the pith where wood characteristics undergo rapid and progressive changes in successive older growth rings from the pith (Larson et al. 2001). According to Clark and Saucier (1989), a radial cross-section of a pine stem typically contains three zones: a core or zone of crown-formed wood, a zone of transition wood, and a zone of mature wood. Both crown-formed wood and transition wood have been commonly referred to as juvenile wood. On that basis, the extent of the juvenile wood region depends on ring number from the pith and proximity to the crown (Larson 1969; Zobel and Sprague 1998). This definition represents the pattern of within-tree variation in successive rings from the pith at a given height (type 2 sequence described by Duff and Nolan 1953); however, it does not consider the botanical phenomenon of maturation or physiological aging in trees, which can be interpreted as an important cause of variation of wood properties in the vertical axis (Burdon et al. 2004*a*, 2004*b*). For this reason, we adopted the concept of transition between corewood and outerwood proposed by Harris and Cown (1991) and Burdon et al. (2004*a*) in this study instead of the traditional concept of transition from

Received 3 January 2006. Accepted 31 August 2006. Published on the NRC Research Press Web site at cjfr.nrc.ca on 20 July 2007.

C.R. Mora[1,2] and H.L. Allen. Department of Forestry and Environmental Resources, North Carolina State University, Raleigh, NC 27695, USA.
R.F. Daniels. Warnell School of Forestry and Natural Resources, The University of Georgia, Athens, GA 30602, USA.
A. Clark. USDA Forest Service, Southern Research Station, Athens, GA 30602, USA.

[1]Corresponding author (e-mail: christian_mora@arauco.cl).
[2]Present address: Bioforest S.A., Casilla 70-C, Concepción, Chile.

 doi:10.1139/X06-250 © 2007 NRC Canada

Table 1. Description of the study sites.

Site	Location	Latitude	Longitude	Region[a]	Annual precipitation (mm)	Planted	Subsoil texture	Drainage
1	Virginia	37°62′N	76°78′W	UACP	1055	1979	Loam	Good
2	North Carolina	35°00′N	78°35′W	LACP	1267	1979	Sandy loam	Poor
3	North Carolina	34°87′N	77°25′W	LACP	1447	1980	Clay loam	Poor
4	South Carolina	33°59′N	79°48′W	LACP	1281	1979	Clay	Poor

[a]UAPC, Upper Atlantic Coastal Plain; LACP, Lower Atlantic Coastal Plain.

juvenile to mature wood. An extensive review of this new conceptual framework can be found in Burdon et al. (2004*a*).

Because of the gradual change in properties with age, the point at which a tree begins producing outerwood is not well defined and varies according to the property being studied (Cown 1992). Properties such as fibre length (Lee and Wang 1996), modulus of rupture, modulus of elasticity, compression strength, and microfibril angle (Bendtsen and Senft 1986; Roos et al. 1990) have been considered to characterize the transition. However, although the demarcation point for each of these characteristics is of scientific interest, we are more concerned with those properties that can be repeatedly and cheaply measured (Sauter et al. 1999). This is the reason why most research into corewood–outerwood transition has been based on wood specific-gravity profiles.

From a practical perspective, the characterization of the transition is needed to understand the effects of silvicultural treatments on wood quality. This allows the comparison between corewood and outerwood properties, the evaluation of management regimes, and the appropriate classification and segregation of the material that will be processed by the industry. For example, Clark et al. (2004) reported that annual weed control plus annual nitrogen fertilization increased the diameter of the corewood 62% in 12-year-old loblolly pine plantations established in the Coastal Plain and Piedmont of Georgia.

Several methods have been used to demarcate core- and outer-wood. The simplest way to identify the region where outerwood starts is to visually locate a point on the specific-gravity curves where the change in the property become less than in the inner corewood as the ring number increases (Bendtsen and Senft 1986; Clark and Saucier 1989) or simply to assign a ring number from the pith at all stem levels, normally 5–15 rings in pines (Hodge and Purnell 1993; Cown and Ball 2001). An alternative approach is to use segmented regression models (Abdel-Gadir and Krahmer 1993; Tassisa and Burkhart 1998) to mathematically determine the demarcation point. The main question is how to estimate this boundary with sufficient reliability (Mutz et al. 2004).

Most of the data used in previous studies consisted of X-ray densitometry pith-to-bark profiles that were collected on trees in observations repeated in time and (or) space. Because data collected from an individual tree tend to be more alike than different, they tend to be correlated, and any two measurements that are closer in time or position are likely to be more closely correlated than two measurements that are more distant. According to Sauter et al. (1999), possible interdependencies in data from adjacent rings could lead to poor estimates of the boundary point, and the use of methods that take into account these interdependencies can lead to estimates with smaller variability. Data of this structure accommodate analysis using mixed-effects modeling techniques, which allow for the inclusion of multiple sources of variation and account for covariate effects with fixed-effects parameters; hence, this method can address corewood in the course of modeling wood properties (Mutz et al. 2004).

According to Burdon et al. (2004*a*), mathematical models that best represent the type 2 sequence of growth are needed to describe the transition from corewood to outerwood. Because loblolly pine shows a pith-to-bark variation dominated by an asymptotic approach to final outerwood values, enough parameters must be included in the model to describe this pattern: the value of the first ring; value of the asymptote; shape of the curve; rate of approach toward the asymptote; and how these parameters are affected by site, genotype, and silviculture.

Established in the late 1970s, the Forest Nutrition Cooperative's regionwide seven installations are the oldest replicated study in the southeastern United States with regionally distributed installations designed to quantify the magnitude and duration of growth and nutritional responses to site preparation, early fertilization, and weed control. These studies provided an excellent opportunity to examine the effects of site and silvicultural treatments on the transition between corewood and outerwood.

The global objective of this study was to fit descriptive curves to pith-to-bark specific gravity profiles of the trees, identifying the data features to be accommodated, the appropriate form of the curves, and the parameters needed for an efficient description. The specific objectives were (*i*) to estimate the demarcation point between corewood and outerwood from X-ray densitometry profiles using a nonlinear mixed-effects model approach accounting for heteroscedasticity, serial correlation of the data, and random variation between samples and (*ii*) to evaluate the effects of early intensive silvicultural treatments on specific-gravity profiles and proportions of corewood and transitional wood produced at breast height (1.3 m).

Materials and methods

Sample origin

Wood samples were obtained from four regeneration trials established by members of the Forest Nutrition Cooperative between 1978 and 1981 in southeastern United States. The sites were located from eastern Virginia to South Carolina (Table 1).

Each field trial received a factorial combination of two levels each of mechanical site preparation (SP), fertilization (F), and herbaceous weed control (H), for a total of eight

© 2007 NRC Canada

treatments per installation. These treatments were applied at establishment in a split-plot design with the two site-preparation treatments comprising the main plots and the 2 × 2 fertilization by weed control factorial being subplots. All trials were initially established with four complete block replicates based on uniformity of soil and site conditions; however, on site 3, one block was dropped because of a fire. Treatment plots were 29 m × 29 m, with 12 rows of 12 seedlings planted at a 2.4 m × 2.4 m spacing (Allen and Lein 1998).

The treatments used in this study were (*i*) control (C); (*ii*) intensive site preparation (SP); (*iii*) intensive site preparation and weed control (SP+H); (*iv*) intensive site preparation and fertilization (SP+F); and (*v*) intensive site preparation, fertilization, and weed control (SP+F+H). The four treatments were progressively more intensive.

Fertilizer treatments included a control (no fertilizer) and diammonium phosphate applied immediately following planting at a rate of 280 kg·ha^{-1} in a 1.2 m wide band centered over the planting row. Weed-control treatments included a control (no herbicides) and a banded (1.2 m) application of hexazinone (Velpar™) applied once during each of the first two growing seasons following planting (rates varied by installation). Site-preparation methods varied by site and interest of the landowner. See Nilsson and Allen (2003) for a complete description of the treatments.

Nine trees from each plot were sampled so as to reflect the diameter distribution of that plot. The number of trees per plot was determined prior to sampling using a power analysis approach for controlling type I (α set to 0.05) and type II ($1 - \beta$ set to 0.80) errors in the statistical hypothesis testing (Cohen 1988).

Wood cores were collected at each site using a 12 mm increment hydraulic borer during the period March–June 2002. Increment cores were taken from each tree at 1.3 m (breast height) above the ground. Trees that were suppressed, atypical in form, or infected by fusiform rust were excluded from sampling. Minor adjustments in sampling height were made to avoid branches and knots. A total of 675 trees were sampled across sites.

According to the classification proposed by Burdon et al. (2004*a*), increment cores taken at breast height would contain "juvenile corewood" and "juvenile transition wood" that would intergrade out from into "juvenile outerwood." However, this "juvenile status" is unlikely to be of appreciable importance for estimating the demarcation point between corewood and outerwood based on ring specific gravity.

Sample preparation and X-ray densitometry analysis

Each core was divided at the pith, and one radial half of each core was prepared for specific gravity data collection. The radial cores were dried at 50 °C for 24 h, glued into yellow poplar (*Liriodendron tupilifera* L.) strips and sectioned along core axes to produce strips of approximately 2 mm thick from the centre of each core exposing transverse faces along the length of the sample. The samples were conditioned to a uniform moisture content of 8% for at least 48 h before they were scanned.

Specific-gravity profiles were obtained from each sample using an X-ray densitometer with a linear resolution of 0.06 mm and a reference standard (calibrated step wedge) was X-rayed along with every sample. The cores were not resin-extracted. The transition from earlywood to latewood was set at a specific-gravity threshold of 0.480 based on green volume and oven-dry mass (Clark et al. 2004). Earlywood and latewood values were weighted according to their sectional areas to obtain whole-ring specific gravity values. The whole-ring specific gravity was then averaged across trees to obtain plot values.

Model formulation and assumptions

Specific gravity shows a consistent general pattern with ring number in loblolly pine. This pattern is characterized by a rapid progression that trails off into a quasi-asymptotic approach to a final set of values with practically no changes beyond rings 16–20 from the pith (Burdon et al. 2004*a*). The specific gravity profiles obtained for each site are shown in Fig. 1.

The original hierarchical structure of the regeneration trials was conserved by grouping the specific gravity data by site, block, and plot. In this three-level grouping structure, level 1 represented the site level, level 2 represented the block level nested within sites, and level 3 corresponded to the plot level nested within blocks and sites. By convention, level 0 represented the population level.

A variety of functions were fitted to the grouped data. After comparing the different models, the four-parameter logistic function was selected as the basic model to represent the specific gravity profiles. The model had the form:

$$[1] \qquad f(\beta, \mathrm{RN}) = \beta_0 + \frac{\beta_1 - \beta_0}{1 + \mathrm{e}^{\left(\frac{(\beta_2 - \mathrm{RN})}{\beta_3}\right)}}$$

where RN was the ring number from the pith, β_0 represented the asymptote as RN $\rightarrow -\infty$, β_1 was the horizontal asymptote as RN $\rightarrow \infty$, β_2 corresponded to the inflection point, and β_3 to the scale parameter (Pinheiro and Bates 2000).

By assuming that y_{ijkl} represented the weighted ring specific gravity of the *k*th plot in the *j*th block of the *i*th site at the *l*th measurement time, the general nonlinear mixed model for specific gravity took the form:

$$[2] \qquad y_{ijkl} = \beta_{0ijk} + \frac{\beta_{1ijk} - \beta_{0ijk}}{1 + \mathrm{e}^{\left(\frac{(\beta_{2ijk} - \mathrm{RN})}{\beta_{3ijk}}\right)}} + \varepsilon_{ijkl}$$

Because there was an interest in how the sites affected specific gravity and not just the specific sites studied, the data were treated as though the four sites were randomly sampled from a large population of sites. The blocks and plots were also considered as randomly sampled from a large population of blocks and plots on each site, thus site-level, block-level, and plot-level effects were random and were expressed as $\mathbf{b}_i$, $\mathbf{b}_{ij}$, and $\mathbf{b}_{ijk}$, respectively, where $i = 1, 2, \ldots, n$ represented the site; $j = 1, 2, \ldots, n_j$ represented the block; $k = 1, 2, \ldots, n_k$ represented the plot; and $l = 1, 2, \ldots, n_{jkl}$ represented the measurement time (ring number). Random site-, block-, and plot-level effects were used to account for site-to-site, block-to-block, and plot-to-plot heterogeneity and implicitly accounted for the within-plot correlation.

© 2007 NRC Canada

Fig. 1. Specific gravity profiles versus ring number from the pith grouped by site.

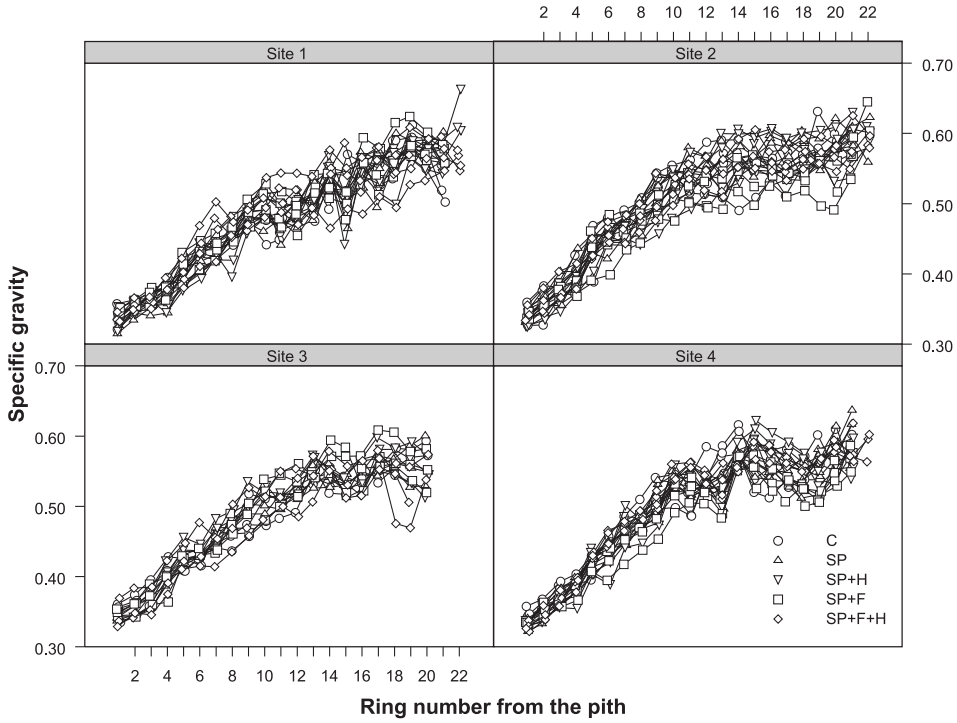

The mixed-effects parameters $\boldsymbol{\beta}_{ijk}$ were expressed as

$$[3] \qquad \boldsymbol{\beta}_{ijk} = \mathbf{A}_{ijk}\boldsymbol{\beta} + \mathbf{B}_{ijk,1}\mathbf{b}_i + \mathbf{B}_{ijk,2}\mathbf{b}_{ij} + \mathbf{B}_{ijk,3}\mathbf{b}_{ijk}$$

where $\mathbf{b}_i$, $\mathbf{b}_{ij}$, and $\mathbf{b}_{ijk}$ were the first-, second- and third-level random-effects vectors; $\mathbf{B}_{ijk,1}$, $\mathbf{B}_{ijk,2}$, and $\mathbf{B}_{ijk,3}$ were the associated random effects design matrices; and $\mathbf{A}_{ijk}$ and $\boldsymbol{\beta}$ were the fixed-effects design matrix and parameter vector, respectively.

The random effects and within-plot error were assumed to be normally distributed as $\mathbf{b}_i \sim N(\mathbf{0}, \boldsymbol{\Psi}_1)$, $\mathbf{b}_{ij} \sim N(\mathbf{0}, \boldsymbol{\Psi}_2)$, $\mathbf{b}_{ijk} \sim N(\mathbf{0}, \boldsymbol{\Psi}_3)$, and $\varepsilon_{ijkl} \sim N(\mathbf{0}, \boldsymbol{\sigma}^2\Lambda_{ijk})$. No constraints were put on $\boldsymbol{\Psi}_1$, $\boldsymbol{\Psi}_2$, and $\boldsymbol{\Psi}_3$ other than assuming that they were variance–covariance matrices.

Which effects should be considered as mixed and which should be considered as fixed in modeling are generally data dependent (Fang and Bailey 2001). The strategy followed to fit the model (eq. 2) began with the inclusion of random effects for all parameters without considering any covariates, and then examining the fit to decide which of the random effects can be eliminated (Pinheiro and Bates 2000; Fang and Bailey 2001). A diagonal structure of the variance–covariance matrices of the random effects ($\boldsymbol{\Psi}_1$, $\boldsymbol{\Psi}_2$, and $\boldsymbol{\Psi}_3$) and an independent matrix of the within-plot errors ($\boldsymbol{\Lambda}_{ijk} = \mathbf{I}_{ijk}$) was assumed initially, to prevent convergence problems with an overparameterized model.

Once the initial fit for the model in eq. 2 was obtained, several reduced models (by dropping one or more random-effect terms) with different structures for the variance–covariance matrices of the estimated random effects were fitted and compared using the log-likelihood ratio test (LRT), the Akaike's information criterion (AIC), and the Schwarz's Bayesian information criterion (BIC), and the model best supported by the data was selected (Davidian and Giltinan 1995).

The next step in the modeling was to trace the random-effects parameters by selecting potentially useful covariates that could explain the random-effects variation. One of the objectives of the original study was to test the effects of silvicultural treatments (considered as fixed effects) on the specific-gravity profiles. The treatments described previously were recoded using dummy variables with I(SP) = 1 if intensive site preparation was included, 0 otherwise; I(F) = 1 if fertilization was included, 0 otherwise; and I(H) = 1 if weed control was included, 0 otherwise. By using this coding, control plots were represented as 0–0–0, and intensive site preparation plus fertilization and weed control plots were represented as 1–1–1. The same approach was applied to account for site effects.

After initial efforts, effects of site 1, site 2, intensive site preparation (SP), and fertilization (F) were taken as fixed to β_{0ijk}; effects of site 1 and site 2 fixed to β_{1ijk}; effects of site 2 fixed to β_{2ijk}; and effects of site 1, site 2, and site 3 fixed to β_{3ijk}. At this point of the model-building strategy, it was clear that the effects of the intensive treatments were minor compared with site effects and were related to variations in the lower asymptote (β_{0ijk}) of the specific-gravity profiles.

Once the covariates and the structure of the matrices of the random effects of the model were defined, the within-plot variance–covariance structure was specified ($\boldsymbol{\Lambda}_{ijk}$). To specify the within-plot variance–covariance structure, both heteroscedasticity and serial correlation structure must be identified. Biological data usually exhibit autocorrelation and heteroscedasticity (Gregoire et al. 1995). The variances of errors around growth models are often found to be de-

© 2007 NRC Canada

pendent on the means; large means usually having larger variance (Fang and Bailey 2001).

Variance functions frequently used in growth modeling are the power model, the exponential model, and the constant power model. These were used to account for heteroscedasticity, represented as $\mathrm{Var}(\varepsilon_{ijkl}) = \sigma^2|\upsilon_{ijkl}|^{2\delta}$, $\mathrm{Var}(\varepsilon_{ijkl}) = \sigma^2 e^{2\delta\upsilon_{ijkl}}$, and $\mathrm{Var}(\varepsilon_{ijkl}) = \sigma^2(\delta_1 + |\upsilon_{ijkl}|^{\delta_2})^2$, respectively. This is a standard way to account for variance that depends systematically on the level of response or some other factor (Davidian and Giltinan 1995). The within-subject autocorrelation was analyzed using several autoregressive models (AR(p)), moving-average models (MA(q)), and mixed autoregressive-moving-average models (ARMA(p,q)). Fits were compared using LRT, AIC, and BIC (Brocklebank and Dickey 1986).

After the addition of covariates into the model and within-plot variance–covariance matrix specification, the assumption of a diagonal structure for the variance–covariance matrices of the estimated random effects was relaxed and several options were compared using LRT, AIC, and BIC criteria.

Demarcation point between corewood and outerwood

The transition from corewood to outerwood in loblolly pine is gradual, and therefore, the extent of juvenile wood and the location of the demarcation point can only be defined by arbitrary criteria (Larson et al. 2001).

Outward from the pith, specific gravity undergoes rapid and progressive changes with increasing ring number. Based on this idea, corewood was defined as the area comprised between ring number 1 and the ring number where the maximum rate of change in specific gravity was observed ($t_{\max}$). The demarcation between transitional wood and outerwood ($t_{\min}$) was arbitrarily defined as the ring at which the rate of change in specific gravity was less than 0.01 units, which for practical purposes represented little change in specific gravity in successive rings, meaning that an stable value of specific gravity was achieved. The area between these two points ($t_{\max}$ and $t_{\min}$) was deemed to represent the transition zone between corewood and outerwood. The amount of corewood was calculated as the ratio between the corewood basal area and total basal area of the trees, using the estimated demarcation point ($t_{\min}$) as the demarcation point between core- and outer-wood at breast height.

After the final model for describing the specific-gravity profiles was fitted, the first derivative with respect to ring number was calculated as

$$[4] \qquad \frac{\mathrm{d}f(\mathrm{RN})}{\mathrm{dRN}} = \frac{\beta_1 - \beta_0}{\beta_3 \times \left(1 + e^{\left(\frac{(\beta_2 - \mathrm{RN})}{\beta_3}\right)}\right)^2} \times e^{\left(\frac{(\beta_2 - \mathrm{RN})}{\beta_3}\right)}$$

Both quantities, the demarcation point and the amount of corewood, were analyzed using a linear model representing the original factorial design of the study of 2 × 2 + 1 control of the form:

$$[5] \qquad y_{ijk} = \mu + \beta_i + \mathrm{SP} + \mathrm{F}_j(\mathrm{SP}) + \mathrm{H}_k(\mathrm{SP}) + \mathrm{FH}_{jk}(\mathrm{SP}) + \varepsilon_{ijk}$$

where y_{ijk} was the proportion of corewood (after Box–Cox transformation; Johnson and Wichern 2002) or the diameter of the juvenile core associated to the levels ith, jth, and kth of the factors, μ was a fixed general mean, β_i was the random effect of the ith block, SP was the fixed effect associated to the control plot, F_j was the fixed effect of the jth level of the fertilizer treatment within the intensive site preparation plot, H_k was the fixed effect of the kth level of the herbicide treatment within the intensive site preparation plot, FH_{jk} was the fixed effect associated to the interaction between the jth level of the fertilizer treatment and the kth level of the herbicide treatment within the intensive site preparation plot, and ε_{ijk} was the random error.

The linear models were fitted using restricted maximum likelihood and the nonlinear models using maximum likelihood, both with SAS option for contrasts in the nlme library version 3.1-65 (Pinheiro et al. 2005) implemented in R version 2.2.0 (R Development Core Team 2005).

Results

Specification of random effects

Several models with different combinations of random and fixed-effects parameters were fitted. Not all models converged. Because reduced models were nested within the full model and they shared the same fixed-effects structure, comparison among the different model formulations was based on LRT statistic. AIC and BIC information criteria were also used to check if the reduction in parameters caused any significant changes in model performance (Table 2).

According to the fit statistics presented on Table 2, model 1 with all parameters considered as mixed (full model) was judged superior and was chosen as the starting model for the description of the specific-gravity profiles. Other combinations of fixed and random effects parameters showed higher AIC and BIC and smaller log-likelihood, indicating that reductions in model specification, at this step, was not appropriate.

Specification of interplot variation

We were interested in determining which covariates were useful in explaining random effects variation. Potential covariates were the intensive silvicultural treatments and the different sites described in the methodology. Each treatment and site were identified as a combination of dummy variables allowing some dimension reduction in the matrices. After several fittings, the final covariate structure of eq. 3 was implemented in model 2 as follows:

$$[6] \qquad \mathbf{A}_{ijk} = \begin{bmatrix} 1 & I(\mathrm{site1}) & I(\mathrm{site2}) & I(\mathrm{SP}) & I(\mathrm{F}) & 0 & 0 & 0 & 0 & 0 & 0 & 0 & 0 & 0 \\ 0 & 0 & 0 & 0 & 0 & 1 & I(\mathrm{site1}) & I(\mathrm{site2}) & 0 & 0 & 0 & 0 & 0 & 0 \\ 0 & 0 & 0 & 0 & 0 & 0 & 0 & 0 & 1 & I(\mathrm{site2}) & 0 & 0 & 0 & 0 \\ 0 & 0 & 0 & 0 & 0 & 0 & 0 & 0 & 0 & 0 & 1 & I(\mathrm{site1}) & I(\mathrm{site2}) & I(\mathrm{site3}) \end{bmatrix}$$

© 2007 NRC Canada

Table 2. Comparison of nonlinear mixed-effects model performance with different random-effects components.

Model	Random effects	Fixed only	No. of parameters	AIC	BIC	Log-likelihood	LRT	*P*
1	$\beta_0,\beta_1,\beta_2,\beta_3$	None	17	–7809.5	–7718.4	3921.8		
1.1	β_0,β_1,β_2	β_3	14	–7760.2	–7685.2	3894.1	55.3	<0.0001
1.2	β_0,β_2,β_3	β_1	14	–7666.3	–7591.2	3847.1	149.3	<0.0001
1.3	β_0,β_1	β_2,β_3	11	–7663.5	–7604.5	3842.8	158.0	<0.0001
1.4	β_1,β_2	β_0,β_3	11	–7722.7	–7663.7	3872.3	98.9	<0.0001
1.5	β_1,β_3	β_0,β_2	11	–7727.4	–7668.5	3874.7	94.1	<0.0001
1.6	β_2,β_3	β_0,β_1	11	–7673.5	–7614.6	3847.8	148.0	<0.0001

Note: AIC, Akaike's information criterion; BIC, Schwarz's Bayesian information criterion; LRT, likelihood ratio test calculated with respect to model 1 (full model).

Table 3. Comparison of nonlinear mixed-effects model performance with the addition of covariates (model 2) and different variance–covariance structures.

Model	Variance function	No. of parameters	AIC	BIC	Log-likelihood	Test	LRT	*P*
2	Homogeneous	24	–7864.5	–7735.8	3956.2			
2.0	Power	25	–8099.5	–7965.5	4074.8	2 vs. 2.0	237.0	<0.0001
2.1	Power (~ring)	25	–8153.5	–8019.4	4101.7			
2.2	Exponential	25	–8090.8	–7956.7	4070.4			
2.3	Exponential (~ring)	25	–8109.6	–7975.5	4079.8			
2.4	Constant power	26	–8097.5	–7958.1	4074.8	2.3 vs. 2.4	10.1	0.0015
2.5	Constand power (~ring)	26	–8151.5	–8012.1	4101.7			

Note: AIC, Akaike's information criterion; BIC, Schwarz's Bayesian information criterion; LRT, likelihood ratio test.

where *I*(site1), *I*(site2), and *I*(site3) were dummy variables used to indicate if observations were from sites 1, 2, or 3, respectively, and *I*(SP) and *I*(F) were dummy variables utilized to indicate the presence or absence of intensive site preparation and fertilization.

Variance function

The homogenous variance assumption of the within-plot residuals in model 2 was checked by plotting the standardized residuals versus fitted values (not shown), indicating that variance increased as the fitted specific gravity values increased. In other words, the inclusion of random-effect terms in the model did not completely rectify the heteroscedasticity observed in the data. Within-plot residuals were defined as the difference between the observed specific gravity and fitted specific-gravity values, conditional on best linear unbiased prediction estimates of the random effects.

According to the information presented in Table 3, all the variance functions utilized resulted in an improvement of the performance of the initial model (model 2), indicating the necessity to account for heteroscedasticity. Considering the AIC and BIC criteria, model 2.1 (power function using ring number as covariate) was the model best supported by the data.

Serial correlation structure

There are a number of alternative parametric models that are commonly used for covariance matrices. One option is to consider explicitly the different sources of variation of the data, i.e., the variation among experimental units (e.g., biological variation) and the variation within experimental units (e.g., due to the way in which the data were collected on the unit). The strategy adopted in this work was to model the two sources of variation together (among and within units), emphasizing the fact that the data were generated over time (Table 4).

The empirical correlation structure for model 2.1 residuals in Table 3 was

$$\begin{aligned}\widehat{\rho} &= [\widehat{\rho}(1), \widehat{\rho}(2), \widehat{\rho}(3), \widehat{\rho}(4), \widehat{\rho}(5), \widehat{\rho}(6)]^T \\ &= [0.137, -0.148, -0.111, -0.009, -0.049, -0.201]^T\end{aligned}$$

where $\widehat{\rho}(l)$ is the empirical autocorrelation calculated at lag l.

A plot of estimated autocorrelation against lags with critical values (α = 0.05) showed that autocorrelations were significant even at six ring-number lags (not shown). For the data examined in this study, the following autoregressive-moving average ARMA(3,2) was the best of the candidate correlation structures based on the statistics presented in Table 4:

$$[7] \qquad \varepsilon_t = \sum_{i=1}^{3} \phi_i \varepsilon_{t-i} + \sum_{j=1}^{2} \theta_j a_{t-j} + a_t$$

where ε_t is the current within-subject error term, ϕ_i are the autoregressive parameters (i = 1, 2, 3), θ_j are the moving-average parameters (j = 1,2), and a_t is a homoscedastic noise term centered at 0 (E[a_t] = 0).

The estimated normalized autocorrelation structure for model 3.8 residuals was

$$\begin{aligned}\widehat{\rho} &= [\widehat{\rho}(1), \widehat{\rho}(2), \widehat{\rho}(3), \widehat{\rho}(4), \widehat{\rho}(5), \widehat{\rho}(6)]^T \\ &= [-0.052, -0.052, -0.063, -0.012, -0.013, -0.101]^T\end{aligned}$$

and the estimated parameters for the ARMA(3,2) model were ϕ_1 = 1.172, ϕ_2 = –0.954, ϕ_3 = 0.337, θ_1 = –0.838, and θ_2 = 0.644.

© 2007 NRC Canada

Table 4. Comparison of nonlinear mixed-effects model performance with different within-plot correlation structures.

Model	Correlation structure	No. of parameters	AIC	BIC	Log-likelihood	Test	LRT	*P*
2.1	Independent	25	–8153.5	–8019.4	4101.7			
3.0	AR(1)	26	–8249.7	–8110.3	4150.9	2.1 vs. 3.0	98.2	<0.0001
3.1	AR(2)	27	–8250.3	–8105.5	4152.1	3.0 vs. 3.1	2.6	0.1076
3.2	MA(1)	26	–8251.9	–8112.4	4151.9	3.1 vs. 3.2	0.4	0.5124
3.3	MA(2)	27	–8251.1	–8106.3	4152.5	3.2 vs. 3.3	1.2	0.2743
3.4	ARMA(1,1)	27	–8251.1	–8106.3	4152.5			
3.5	ARMA(1,2)	28	–8254.9	–8104.8	4155.5	3.4 vs. 3.5	5.9	0.0151
3.6	ARMA(2,1)	28	–8249.1	–8098.9	4152.6			
3.7	ARMA(2,2)	29	–8253.6	–8098.1	4155.8	3.6 vs. 3.7	6.4	0.0112
3.8	ARMA(3,2)	30	–8271.3	–8110.4	4165.6	3.7 vs. 3.8	19.7	<0.0001

Note: AR(*p*), autoregressive correlation structure of order *p*; ARMA (*p*,*q*), autoregressive-moving average correlation structure of order *p*,*q*; MA (*q*), moving average correlation structure of order *q*; AIC, Akaike's information criterion; BIC, Schwarz's Bayesian information criterion; LRT, likelihood ratio test.

Final model structure and parameter estimation

After the specification of which parameters should be considered as mixed or purely fixed, the covariate structure, and the variance and correlation functions, the assumption of a diagonal distribution of the estimated random-effects matrices was relaxed, and model 3.8 was refitted. In the final model (model 4), Ψ_1 (the variance component of the random effects at the site level), was represented as an unstructured matrix between $b_i^{(2)}$ and $b_i^{(3)}$; Ψ_2 (the block level) was reduced to $b_{ij}^{(3)}$ term; and Ψ_3 (the plot-replicate level) was represented as an unstructured matrix between $b_{ijk}^{(1)}$, $b_{ijk}^{(2)}$, and $b_{ijk}^{(3)}$. Thus, the final model to describe the specific gravity profiles was expressed as

$$[8] \qquad y_{ijk} = f(\mathrm{RN}, \beta_{ijk}) + \varepsilon_{ijk}$$

$$y_{ijkl} = \beta_{0ijk} + \frac{\beta_{1ijk} - \beta_{0ijk}}{1 + \mathrm{e}^{\left(\frac{(\beta_{2ijk} - \mathrm{RN})}{\beta_{3ijk}}\right)}} + \varepsilon_{ijkl}$$

$$\beta_{0ijk} = \Big(\beta_{00} + \beta_{01} \times I(\mathrm{site1}) + \beta_{02} \times I(\mathrm{site2}) + \beta_{03} \times I(\mathrm{SP}) + \beta_{04} \times I(\mathrm{F})\Big)$$

$$\beta_{1ijk} = \Big(\beta_{10} + \beta_{11} \times I(\mathrm{site1}) + \beta_{12} \times I(\mathrm{site2}) + b_{ijk}^{(1)}\Big)$$

$$\beta_{2ijk} = \Big(\beta_{20} + \beta_{21} \times I(\mathrm{site2}) + b_i^{(2)} + b_{ijk}^{(2)}\Big)$$

$$\beta_{3ijk} = \Big(\beta_{30} + \beta_{31} \times I(\mathrm{site1}) + \beta_{32} \times I(\mathrm{site2}) + \beta_{33} \times I(\mathrm{site3}) + b_i^{(3)} + b_{ij}^{(3)} + b_{ijk}^{(3)}\Big)$$

$$\varepsilon_{ijkl} \sim (0, \sigma^2 \mathbf{\Lambda}_{ijk})$$

$$\sigma^2 \mathbf{\Lambda}_{ijk} = \sigma^2 G_{ijk}^{1/2}(\beta_{ijk}, \delta)\Gamma_{ijk}(\phi, \theta) G_{ijk}^{1/2}(\beta_{ijk}, \delta)$$

$$G_{ijk}(\beta_{ijk}, \delta) = |\mathrm{RN}|^{\delta}$$

$$\Gamma_{ijk}(\phi, \theta) = \mathrm{ARMA}(3, 2)$$

$$\mathbf{b}_i = \left(b_i^{(2)}, b_i^{(3)}\right)^T$$

$$\mathbf{b}_{ij} = b_{ij}^{(3)}$$

$$\mathbf{b}_{ijk} = \left(b_{ijk}^{(1)}, b_{ijk}^{(2)}, b_{ijk}^{(3)}\right)^T$$

where $G_{ijk}(\beta_{ijk}, \delta)$ is the variance function, δ is the parameter associated to the variance function (which has a value of 0.498), and $\Gamma_{ijk}(\phi, \theta)$ is the serial correlation function. The remaining elements of the model have been described previously.

Parameter estimates and corresponding standard errors and *P* values for the fixed effects of model 4 (eq. 8) are given in Table 5. A graphical representation of the population response (level 0) was obtained by setting the random effects estimates of $b_{ijk}^{(1)}$, $b_i^{(2)}$, $b_{ijk}^{(2)}$, $b_i^{(3)}$, $b_{ij}^{(3)}$ and $b_{ijk}^{(3)}$ to zero, and plugging in the corresponding fixed-effects values into eq. 8 (Fig. 2).

Intensive silvicultural treatments shared identical estimates of the parameters β_1 (upper asymptote), β_2 (inflection point), and β_3 (scale parameter) within each site; however, differences associated with site preparation and fertilization were observed on the lower asymptote (β_0), which had smaller values than control plots in all sites.

The upper asymptote ranged from 0.563 to 0.583 with the smallest values observed on sites 3 and 4. The lower asymp-

© 2007 NRC Canada

Table 5. The estimated fixed effects for population prediction (random effects set to 0) for the nonlinear mixed-effects specific gravity model (df = 1488 throughout).

Parameter	Definition[a]	Value	SE	t	P
β_{00}	Population mean intercept – LA	0.203	0.017	11.64	<0.0001
β_{01}	Effect of site 1 – LA	0.051	0.010	5.05	<0.0001
β_{02}	Effect of site 2 – LA	0.036	0.016	2.33	0.0197
β_{03}	Effect of site preparation – LA	0.013	0.004	3.51	0.0005
β_{04}	Effect of fertilization – LA	–0.006	0.003	–2.05	0.0406
β_{10}	Population mean intercept – UA	0.596	0.010	61.69	<0.0001
β_{11}	Effect of site 1 – UA	–0.019	0.008	–2.29	0.0221
β_{12}	Effect of site 2 – UA	–0.013	0.006	–2.21	0.0272
β_{20}	Population mean intercept – IP	4.583	0.331	13.85	<0.0001
β_{21}	Effect of site 2 – IP	0.943	0.368	2.56	0.0106
β_{30}	Population mean intercept – RC	6.110	0.471	12.96	<0.0001
β_{31}	Effect of site 1 – RC	–2.150	0.367	–5.85	<0.0001
β_{32}	Effect of site 2 – RC	–0.672	0.295	–2.28	0.0226
β_{33}	Effect of site 3 – RC	–0.474	0.124	–3.81	0.0001

[a]LA, lower asymptote (β_{0ijk}); UA, upper asymptote (β_{1ijk}); IP, inflection point (β_{2ijk}); RC, rate of change (β_{3ijk}).

Fig. 2. Population specific gravity profiles where all random effects were set equal to zero.

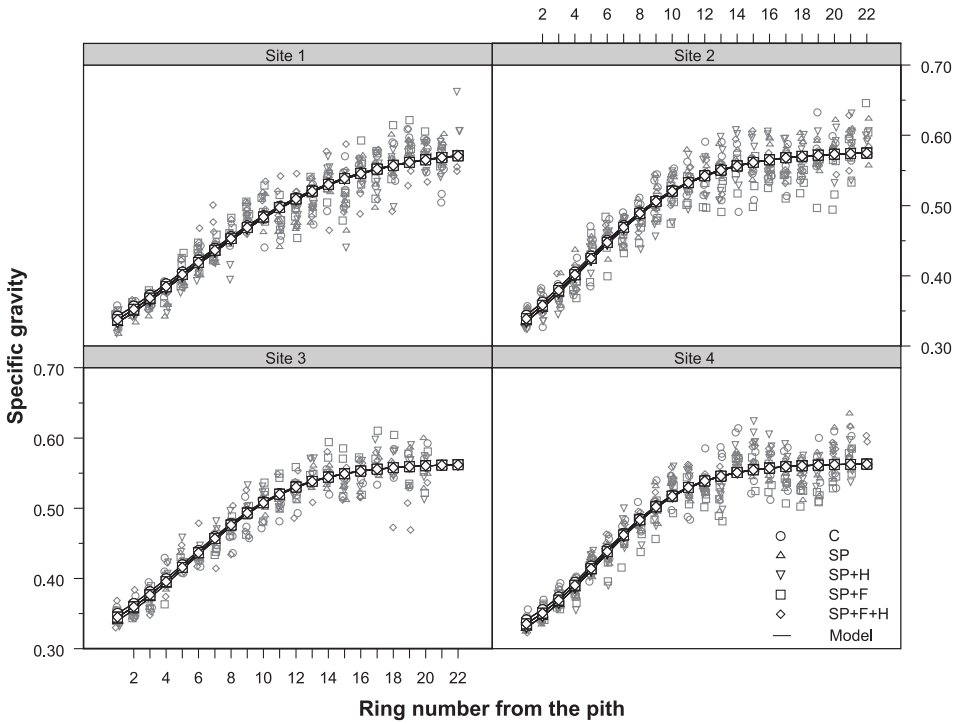

tote ranged from 0.233 to 0.296 with the smallest value observed on site 1 and higher values on sites 3 and 4. The inflection point was almost the same for all sites (5.5 years) except for site 2, in which the inflection point was 4.6 years. The inflection point can be thought of as the ring number when the response is $(\beta_1-\beta_0)/2$, i.e., halfway between the lower and upper asymptote. The scale parameter on the x axis showed the greatest variation among sites, ranging from 2.81 on site 4 up to 4.96 on site 1. This parameter plus the inflection point (β_2) can be interpreted as the ring number when the response is roughly three-quarters of the distance between the lower and the upper asymptote.

No significant departures from the assumption of normality for the within-plot errors were observed in the normal probability plot of the standardized residuals as shown in Fig. 3.

A final assessment of the adequacy of model 4 is given by the plot of the augmented predictions (Pinheiro and Bates 2000) for a randomly chosen subset of the data (Fig. 4). For comparison, both the population predictions and the within-plot predicitions are displayed.

Demarcation point, diameter of the juvenile core, and proportion of corewood

The estimated demarcation point ($t_{\min}$) and transition zone (segment of the curve between $t_{\max}$ and $t_{\min}$), calculated as a function of the four parameters of the logistic model (eq. 4) are given in Table 6.

© 2007 NRC Canada

Fig. 3. Normal plot of standardized residuals for the model 4.

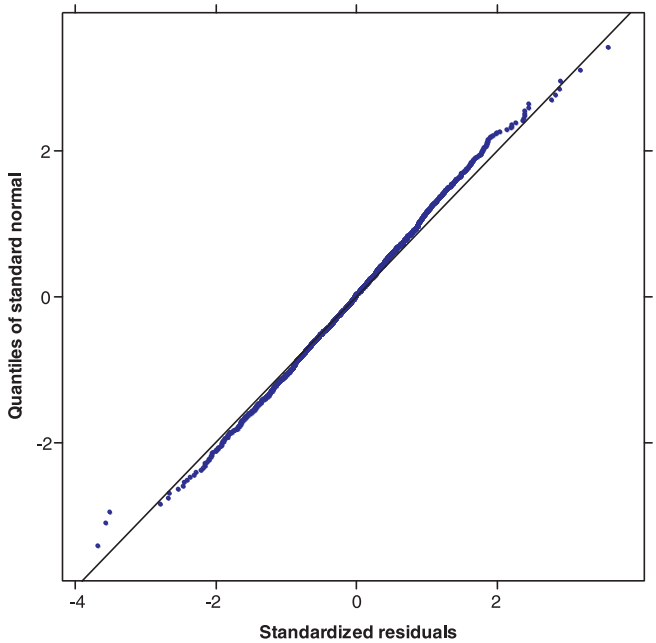

Across sites, the transition zone between corewood and outerwood were located between rings 5 and 15. No effects on either demarcation point were associated with the silvicultural treatments. The variation of both quantities was explained by differences in site conditions, as showed previously during the specification of the interplot variation matrix. The highest demarcation point was observed on site 1 (ring 15), and the lowest (12) was observed on site 4. Sites 1, 3, and 4 initiated the transition zone at ring 6, whereas site 2 initiated it at ring 5.

The demarcation point ($t_{\min}$) was used to determine the diameter of the juvenile core (DJC). An increase of DJC was observed in all sites as a result of the early intensive treatments, except for site 3. When combined, the treatments increased DJC by 15%, 12%, and 9% over control plots on sites 1, 2, and 4, respectively. On site 3, the treatments decreased DJC in 9% compared with control plots. A formal analysis of variance (based on eq. 5 showed a significant effect ($P < 0.01$) of SP and H on DJC on site 1, which increased as the intensity of the treatments increased. A significant effect of SP was found on site 2, which increased the mean DJC of the treated plots in 12% compared with the mean DJC of the control plots. On sites 3 and 4, no significant effects of SP, F, or H were observed on the mean values of DJC (Table 7).

In terms of the percentage of corewood produced at breast height, the analysis showed that site preparation, fertilization, and herbicide did not statistically affect the amount of corewood on sites 1, 3, and 4 (Table 7). A statistically significant effect ($P < 0.01$) was associated with fertilizer application within the intensive treatments on site 2. The fertilizer treatment decreased the mean percentage of corewood, 61% for SP+F and SP+F+H compared with 65% for SP and SP+H. It is worth noting that this effect is not evident when the SP+F and SP+F+H treatments are compared with control plots.

Combining all treatments (SP, SP+H, SP+F, and SP+F+H), the mean percentage of corewood varied from 55% on site 4 to 75% on site 1, indicating a trend with geographic location, with the lowest amount observed in the site located in South Carolina (site 4) and the highest observed in Virginia site 1). On site 1, the mean percentage of corewood of the treatments was the same of that observed in control plots (75%). On site 2, silvicultural treatments resulted in a mean of 63% of corewood, 3% higher than control plots. A small variation was observed on site 3, for which the mean percentage of corewood was 65% and 64% for treatments and control plots, respectively. Finally, on site 4, an increase of 2% was associated with early intensive silviculture compared with control plots. In all cases, the mean percent corewood of the treatments (at breast height) was not statistically different from the values showed by control plots.

Discussion

The methodology presented in this paper for modeling pith-to-bark specific gravity profiles is especially appropriate when the aim of the study is to describe a response variable by fitting a mathematical model, because growth curves (a statistical term that refers to the situation where the same characteristic is observed at different times or locations on the same subjects) are usually nonlinear with growth approaching an asymptote. Fit, parsimony, and parameter interpretability are among the advantages of nonlinear models over linear ones.

Mixed-effects models are useful tools for analyzing longitudinal data, as in ring sequences. They present an inherent flexibility that allows for development of a unique variance–covariance structure, which overcomes a limitation in traditional nonlinear regression (Hall and Clutter 2004). By fitting a nonlinear regression model of the form presented in eq. 8, we accounted for the statistical sources of variation that could have affected the specific-gravity profiles of individual plots within and among sites. However, the selection of an appropriate correlation structure and variance function is data dependent, so a generalization of these two particular structures to other data sets is not guaranteed. If the true covariance structure is simpler than that presented here, then no improvement will be obtained by specifying more complicated models, and tests can lack power.

The criterion selected for estimating the demarcation point was arbitrary and may be arguable. However, it has the advantage that it represents a position on the fitted curves that can be accurately defined in terms of the parameters of the models. The threshold value of 0.01 for the increment of specific gravity in successive rings utilized in this study to define the point that leads to a stable value of specific gravity (indicator of the presence of outerwood) was chosen to assure that differences in specific gravity below this point did not have an impact on the quality of the material evaluated. Mitchell (1964) reported that differences of 0.02 units of specific gravity can lead to differences of 50 lb. (1 lb. = 0.454 kg) in pulp yield per ton (1 ton = 0.907 t) of roundwood.

Previous works have focused on determining the demarcation point between corewood and outerwood using latewood

© 2007 NRC Canada

Fig. 4. Population predictions (fixed), within-group predictions (curves), and observed specific gravity values (circles) versus ring number for a subset of data (values on the top of each subplot correspond to site/block/plot combination).

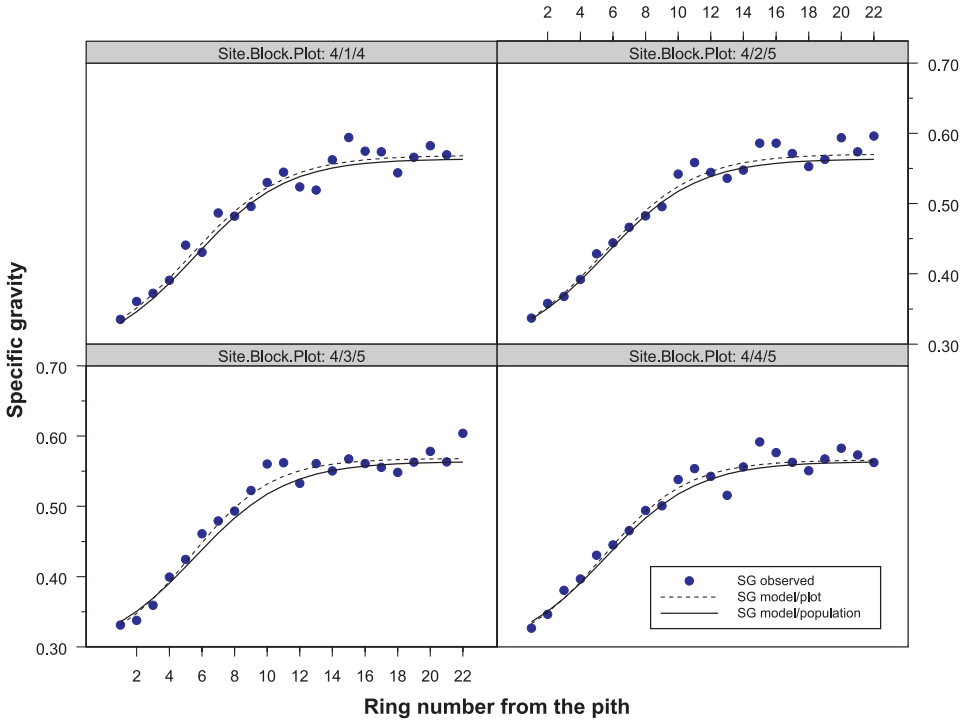

Table 6. Estimated demarcation points for corewood (t_{max}), outerwood (t_{min}) and transition zone (t_{max}–t_{min}) obtained for each site.

	Ring No.		
Site	t_{max}	t_{min}	t_{max}–t_{min}
1	6	15	6–15
2	5	13	5–13
3	6	13	6–13
4	6	12	6–12

specific gravity only or some other wood property. We selected specific gravity because, as Megraw (1985) pointed out, in annual-ring specific gravity three seasonal components converge: earlywood specific gravity, latewood specific gravity, and the percentage of each of them. By modeling specific gravity we are not excluding any of these three elements. Moreover, it has been demonstrated that specific gravity is closely related to the quality of the end products and is a property that is easy to measure.

Small differences in the position of the transition zone within plots were found among sites. In general, the transition zone between corewood and outerwood was located between rings 5 and 15 (Table 6). On site 4, located in South Carolina, the demarcation point between the two types of wood was reached earlier (ring 12) than in the other three sites, and this position was continuously increasing as we moved north, where the demarcation point was reached at ring 15 corresponding to the site 1 located in eastern Virginia. This geographical trend in specific gravity has been reported previously in loblolly pine (Talbert and Jett 1981; Zobel and van Buijtenen 1989), where trees on sites located in the southern United States tend to have higher specific gravity compared with sites located further north because of differences in site and climate conditions, characteristics that may be associated with the time required for the trees to reach corewood specific-gravity values.

The time in which the trees began producing transitional wood was the same for all sites (ring 6) except for site 2, where it commenced a year earlier. This difference is probably associated with the fixed effect of site 2 on the scale parameter (β_3) of the specific gravity model (eq. 8).

There were no significant treatment effects on the transition zone and demarcation point at any site, indicating that the intensive silvicultural treatments applied on the study sites did not affect the ring number at which the trees began generating outerwood. This is an interesting result, especially considering that some treatments effects (SP and F) were observed on the lower asymptote (β_0) of the specific-gravity model. This effect may be the result of a short-term effect of the treatments in specific gravity on the first couple of rings, and since no differences were observed on the remaining parameters of the model, we may conclude that intensive treatments applied at time of planting can result on small differences in wood quality during the first couple of years following the application, but then they tend to disappear. Similarly, Clark and Edwards (1999) reported no effects of different site-preparation treatments on transition age, which averaged 10 years for all treatments. Tassisa and Burkhart (1998) found no effects of different thinning schemes on the demarcation point, which was estimated to occur at approximately ring 11 or 12 from the pith.

Considering the demarcation points estimated, a mean increase of the DJC up to 15%, as a result of the silvicultural treatments was observed among sites in this study (Table 7). Analysis of growth data (Forest Nutrition Cooperative 1996)

© 2007 NRC Canada

Table 7. Estimated percentage of corewood and diameter of the juvenile core for each site-treatment combination.

Variable and treatment	Site 1	2	3	4
Corewood (%)				
C	74.5*ab*	60.1*c*	63.7*a*	52.3*a*
SP	76.2*a*	64.4*ab*	63.4*a*	56.6*a*
SP+H	72.6*b*	65.1*a*	63.8*a*	57.0*a*
SP+F	75.5*ab*	59.4*c*	69.8*a*	54.9*a*
SP+F+H	73.6*ab*	61.8*bc*	63.8*a*	52.8*a*
Diameter of the juvenile core (cm)				
C	14.8*c*	15.4*b*	18.9*a*	12.8*b*
SP	15.9*b*	17.1*ab*	15.2*b*	14.0*ab*
SP+H	17.8*a*	17.4*a*	17.3*ab*	13.3*ab*
SP+F	16.2*b*	17.6*a*	17.7*ab*	14.7*a*
SP+F+H	18.1*a*	17.1*a*	18.6*a*	13.8*ab*

Note: Within each site–variable combination, values with different letters are significantly different from each other (LSD test at $\alpha = 0.05$). Treatments are as follows: C, control; SP, site preparation; F, fertilization; H, herbicide.

Table 8. Standing volume per hectare ($m^3 \cdot ha^{-1}$), 14 years after planting, for the different site–treatment combinations.

Treatment	Site 1	2	3	4
C	116	127	174	68
SP	134	192	163[a]	126
SP+H	117	226	191	127
SP+F	147	175	216	138
SP+F+H	168	196	248	141

Note: See Table 7 for treament abbreviations.

[a]Intensive site preparation on site 3 involved piling prior bedding which had a negative effect on individual tree growth when applied without fertilizer or weed control.

showed differences in standing volume at 14 years between control plots (low site preparation) and intensive treatment plots (Table 8). This means that, even when the transition between corewood and outerwood involved the same ring numbers for all treatments within each site, differences in growth among individual trees at the same age resulted in higher DJC for some treatments plots.

The types of long-term growth response to early silvicultural treatments vary according to the treatments applied and site characteristics. Site-preparation and weed-control treatments typically result in growth gains achieved early in the rotation that are either maintained or partially lost by harvest. Fertilization, on the other hand, may result in either short- or long-term increases in nutrient availability and increased growth depending on site and soil conditions (Morris and Lowery 1988). In this study, intensive silvicultural treatments applied at the time of planting did increase the diameter of the juvenile core. However, they also increased the size of the trees by the end of the measurement period, indicating that gains achieved during the early years were maintained until the age of the trees in this study. The relationship between the size of DJC and the size of the diameter at breast height of the trees was analyzed in terms of their corresponding basal areas, because as Zobel and Sprague (1998) pointed out, interest in the amount of corewood ultimately relates to how much of the merchantable volume is under this condition.

The results presented in Table 7 showed that, in the worst scenario, the proportion of corewood at breast height was increased by the treatments in 3% compared with control plots. In all cases, the increase observed was not statistically significant ($P > 0.05$). The proportion of corewood followed the same trend as the specific gravity and as the demarcation point, i.e., increasing as we moved from the south to the north.

Therefore, if the main concern is the amount corewood present as a result of silvicultural treatments, the comparison must be based on the size of the basal area of corewood with respect to the final basal area of the trees and not on the size of the juvenile core alone. Of course, this comparison will be valid only for trees of the same age. Similar results are reported by Saucier and Cubbage (1990) and Zobel and van Buijtenen (1989) who found a larger diameter of juvenile corewood in more widely spaced pine plantations but a lesser percentage of the total volume of the tree.

Large differences in growth during early years associated with site preparation and fertilization, herbicide, and fertilization plus herbicide resulted in a larger DJC on site 2 for those treatments (Tables 7 and 8). No thinning was done on this site, and treatment differences in diameter found during the early years were not observed at sampling age, resulting in trees with higher proportion of juvenile corewood in some cases compared with control trees. This suggests that treatment effects on the patterns of growth with age are critically important in determining the proportion of corewood.

In conclusion, site preparation, fertilization, and weed control applied at establishment had only a modest effect on the amount of juvenile corewood, which agrees with the information reported by Zobel and Sprague (1998). The results suggested that where strong growth responses to fertilization and weed control were observed, the proportion of corewood was not affected; in addition, when the strong growth responses were related to weed control, either by a mechanical control in the case of site preparation alone or chemical control, the transition age tend to increase in intensive silvicultural plots compared with control plots. Because trees under intensive management will likely reach merchantable sizes at younger ages, a trade-off between the amount of corewood obtained and the most economical time to harvest must be considered as an important factor determining the presence or absence of cultural effects on wood quality of loblolly pine.

Acknowledgements

The authors gratefully acknowledge support from the Forest Nutrition Cooperative of the North Carolina State University and Virginia Polytechnic Institute and State University, the Wood Quality Consortium of the University of Georgia, and the USDA Forest Service Southern Research Station. We also like to recognize and thank Rowland D. Burdon from Ensis and R. James Barbour from Focused Science Delivery for their helpful comments in reviewing

© 2007 NRC Canada

the manuscript. Christian Mora would also like to thank Bailian Li and David Dickey from the North Carolina State University and Miguel Peredo from Bioforest S.A. for the support given to complete this work.

References

Abdel-Gadir, A.Y., and Krahmer, R.L. 1993. Estimating the age of demarcation of juvenile and mature wood in Douglas-fir. Wood Fiber Sci. **25**: 242–249.

Allen, H.L., and Lein, S. 1998. Effects of site preparation, early fertilization, and weed control on 14-year old loblolly pine. Proc. South. Weed. Sci. Soc. **51**: 104–110.

Bendtsen, B.A., and Senft, J. 1986. Mechanical and anatomical properties in individual growth rings of plantation-grown eastern cottonwood and loblolly pine. Wood Fiber Sci. **18**: 23–38.

Brocklebank, J.C., and Dickey, D.A. 1986. SAS system for forecasting time series. 1986 ed. SAS Series in Statistical Applications. SAS Institute Inc., Cary, N.C.

Burdon, R.D., Kibblewhite, R.P., Walker, J.C.F., Megraw, R.A., Evans, R., and Cown, D.J. 2004*a*. Juvenile versus mature wood: a new concept, orthogonal to corewood versus outerwood, with special reference to *Pinus radiata* and *P. taeda*. For. Sci. **50**: 399–415.

Burdon, R., Walker, J., Megraw, B., Evans, R., and Cown, D. 2004*b*. Juvenile wood (*sensu novo*) in pine: conflicts and possible opportunities for growing, processing and utilization. N.Z. J. For. **49**: 24–31.

Clark, A., III, and Edwards, M.B. 1999. Effect of six site-preparation treatments on Piedmont loblolly pine wood properties at age 15. *In* Proceedings of the 10th Biennal Southern Silvicultural Research Conference, 16–18 Feb. 1999, Shreveport, La. USDA For. Serv. South. Res. Stn. Gen. Tech. Rep. GTR-SRS-30. pp. 316–320.

Clark, A., III, and Saucier, J.R. 1989. Influence of planting density, intense culture, geographic location, and species on juvenile wood formation in southern pine. For. Prod. J. **39**: 42–48.

Clark, A., III, Borders, B., and Daniels, R. 2004. Impact of vegetation control and annual fertilization on properties of loblolly pine wood at age 12. For. Prod. J. **54**: 90–96.

Cohen, J. 1988. Statistical power analysis for the behavioral sciences. 2nd ed. Lawrence Erlbaum Associates, Inc., Hillsdale, N.J.

Cown, D.J. 1992. Corewood (juvenile wood) in *Pinus radiata*—should we be concerned? N.Z. J. For. Sci. **22**: 87–95.

Cown, D.J., and Ball, R.D. 2001. Wood densitometry of 10 *Pinus radiata* families at seven contrasting sites: influence of tree age, site, and genotype. N.Z. J. For. Sci. **31**: 88–100.

Davidian, M., and Giltinan, D.M. 1995. Nonlinear models for repeated measurement data. Monogr. Stat. Appl. Prob. 62. Chapman & Hall/CRC Press.

Duff, G.H., and Nolan, N.J. 1953. Growth and morphogenesis in the Canadian forest species. 1. The controls of cambial and apical activity in *Pinus resinosa.* Can. J. Bot. **13**: 471–513.

Fang, Z., and Bailey, R.L. 2001. Nonlinear mixed effects modeling for slash pine dominant height growth following intensive silvicultural treatments. For. Sci. **47**: 287–300.

Forest Nutrition Cooperative. 1996. Effects of site preparation and early fertilization and weed control on 14-year loblolly pine growth. Forest Nutrition Cooperative, Department of Forestry, North Carolina State University, Raleigh, N.C. NCSFNC Rep. 36.

Gregoire, T.G., Schabenberger, O., and Barret, J.P. 1995. Linear modeling of irregularly spaced, unbalanced, longitudinal data from permanent-plot measurements. Can. J. For. Res. **25**: 137–156.

Hall, D.B., and Clutter, M. 2004. Multivariate multilevel nonlinear mixed effects model for timber yield predictions. Biometrics, **60**: 16–24. doi:10.1111/j.0006-341X.2004.00163.x. PMID:15032769.

Harris, J.M., and Cown, D.J. 1991. Basic wood properties. *In* Properties and uses of New Zealand radiata pine. Vol. 1. Wood properties. *Edited by* J.A. Kininmonth and L.J. Whitehouse. Ministry of Forestry, Forest Research Institute, Rotorua, N.Z. pp. 6-1 – 6-28.

Hodge, G.R., and Purnell, R.C. 1993. Genetic parameter estimates for wood density, transition age, and radial growth in slash pine. Can. J. For. Res. **23**: 1881–1891.

Johnson, R.A., and Wichern, D.W. 2002. Applied multivariate statistical analysis. 5th ed. Prentice Hall, Upper Saddle River, N.J.

Larson, P.R. 1969. Wood formation and the concept of wood quality. Yale. Univ. Sch. For. Bull. 74.

Larson, P.R., Kretschmann, D.E., Clark, A., III, and Isebrands, J.G. 2001. Formation and properties of juvenile wood in southern pines: a synopsis. USDA For. Serv. For. Prod. Lab. Gen. Tech. Re. FPL-GTR-129.

Lee, C.H., and Wang, S.Y. 1996. A new technique for the demarcation between juvenile and mature wood in *Cryptomeria japonica*. IAWA J. **17**: 125–131.

Megraw, R.A. 1985. Wood quality factors in loblolly pine. The influence of tree age, position in tree, and cultural practice on wood specific gravity, fiber length, and fibril angle. Tappi Press, Atlanta, Ga.

Mitchell, H. 1964. Patterns of variation in specific gravity of southern pines and other coniferous species. Tappi J. **47**: 276–283.

Morris, L.A., and Lowery, R.F. 1988. Influences of site preparation on soil conditions affecting stand establishment and tree growth. South. J. Appl. For. **12**: 170–178.

Mutz, R., Guilley, E., Sauter, U.H., and Nepveu, G. 2004. Modeling juvenile–mature wood transition in Scots pine (*Pinus sylvestris* L.) using nonlinear mixed-effects models. Ann. For. Sci. **61**: 831–841. doi:10.1051/forest:2004084.

Nilsson, U., and Allen, H.L. 2003. Short- and long-term effects of site preparation, fertilization, and vegetation control on growth and stand development on planted loblolly pine. For. Ecol. Manage. **175**: 367–377. doi:10.1016/S0378-1127(02)00140-8.

Pinheiro, J.C., and Bates, D.M. 2000. Mixed-effects models in S and S-Plus. Springer Series in Statistics and Computing. Springer-Verlag, New York.

Pinheiro, J., Bates, D., DebRoy, S., Sarkar, D. 2005. nlme: linear and nonlinear mixed effects models. R package, Version 3.1-65.

Plomion, C., Leprovost, G., and Stokes, A. 2001. Wood formation in trees. Plant Physiol. **127**: 1513–1523.

R Development Core Team. 2005. R: a language and environment for statistical computing. R Foundation for Statistical Computing, Vienna. Available from www.R-project.org [accessed 3 January 2006].

Roos, K.D., Shottafer, J.E., and Shepard, R.K. 1990. The relationship between selected mechanical properties and age in quaking aspen. For. Prod. J. **70**: 54–56.

Saucier, J.R, and Cubbage, F.W. (*Editors*). 1990. Forest management and wood quality. *In* Proceedings of Southern Plantation Wood Quality Workshop, 6–7 June 1989, Athens, Ga. USDA For. Serv. Gen. Tech. Rep. SE-63. pp. 47–56.

Sauter, U.H., Mutz, R., and Munro, B.D. 1999. Determining juvenile–mature wood transition in Scots pine using latewood density. Wood Fiber Sci. **31**: 416–425.

Talbert, J.T., and Jett, J.B. 1981. Regional specific gravity values for plantation grown loblolly pine in the southeastern United States. For. Sci. **27**: 801–807.

Tassisa, G., and Burkhart, H.E. 1998. Juvenile–mature wood demarcation in loblolly pine trees. Wood Fiber Sci. **30**: 119–127.

© 2007 NRC Canada

Zobel, B.J., and Sprague, J.R. 1998. Juvenile wood in forest trees. Springer Series in Wood Science. Springer-Verlag, New York.
Zobel, B.J., and van Buijtenen, J.P. 1989. Wood variation: its causes and control. Springer Series in Wood Science. Springer-Verlag, New York.

© 2007 NRC Canada